

MAPPING VEGETATION COVERAGE IN THE BUILT-UP AREA OF LUOYANG, CHINA, FROM THE PERSPECTIVE OF THE TOURISM DEMAND

WANG, S.^{1,2} – KADYROVNA, K. M.² – LIU, H. P.^{1*}

¹*School of Geography and Tourism, Luoyang Normal University, Luoyang, Henan Province
471934, China*

²*Institute of Management and Business, Kyrgyz National University named after Jusup
Balasagyn, Bishkek 720033, Kyrgyzstan*

**Corresponding author
e-mail: gatestudy@163.com*

(Received 10th Oct 2023; accepted 9th Feb 2024)

Abstract. Mapping the vegetation coverage in a world-famous city provides a reference for tourists to initially experience the city. Luoyang, China, is a world-famous tourist city, and many tourists want relevant information on the vegetation coverage so that they can review the city's greening conditions before travelling. In this study, we used Landsat-8 images from 2021 as the data source to extract the normalized difference vegetation index (NDVI), used the NDVI dimidiated pixel model to obtain vegetation coverage images, removed blue ground objects in the images and conducted classification. Next, transformation analysis was performed of classification maps of different vegetation coverage levels in summer and winter. The results showed that the vegetation coverage area within the built-up area in summer was approximately 243.12 km² (67.71%), whereas that in winter reached approximately 216.43 km² (60.27%). Regardless of the season, the higher the vegetation coverage level is, the smaller the occupied area. Compared to those in summer, the types of high vegetation cover decreased in winter, and they shifted towards lower vegetation cover types. According to the experimental results, the vegetation coverage area in Luoyang is very large in summer, and although it slightly decreases in winter, it still occupies a large proportion of the total area. This indicates that tourists can enjoy large-scale vegetation in Luoyang.

Keywords: *world-famous tourist city, built-up area of Luoyang, vegetation coverage mapping, dimidiated pixel model, summer and winter seasons*

Introduction

In the tourist cities of northern China, the temperature is very high in summer. Before travelling, tourists want to know if the destination city exhibits suitable vegetation coverage conditions because a high vegetation coverage suggests that the city can provide a satisfactory cooling effect. In winter, most trees in northern Chinese cities shed their leaves, and tourists want to know whether there are still green plants because grey cities without green plants could affect the mood. Therefore, vegetation coverage mapping of tourist cities can provide basic information on vegetation greening in specific cities for tourists to help them consider drought/wetness, cold/heat, aesthetics, and degree of landscape harmony of target cities (Luo, 2019; Zhang et al., 2022a). Therefore, from the perspective of the demand of tourists for urban green space information, mapping the vegetation coverage in well-known tourist cities and collecting relevant data have become focal points in existing research (Li et al., 2019; Liu et al., 2022a). In addition, vegetation coverage mapping can provide city planners with important information regarding the state of urban greening so that they can

implement appropriate urban management measures to promote or maintain the urban vegetation coverage conditions to meet the needs of tourists for large-scale vegetation coverage (Huang et al., 2011; Wang et al., 2023). To realize urban vegetation coverage mapping for tourism needs, we can obtain detailed information on urban vegetation coverage through satellite remote sensing images with high spatial resolution, urban topographic maps and vegetation survey data.

At present, the methods used for mapping the vegetation coverage in a target area are based on the classification of remote sensing images, establishment of monitoring models and use of the spectral index method (Liu et al., 2022b). Remote sensing images can be employed to distinguish and characterize different types of vegetation. The commonly used classification methods include supervised and unsupervised classification methods (Du et al., 2022). The monitoring model method entails the use of remote sensing data and ground observation data to establish mathematical models to monitor the vegetation coverage (Zhang et al., 2022b). The commonly used monitoring models include regression models, support vector regression models and neural networks (Zhang et al., 2022b). The spectral index method uses vegetation indices from remote sensing data to evaluate the vegetation coverage (Yu et al., 2023). Commonly adopted vegetation indices include the normalized difference vegetation index (NDVI) and the enhanced vegetation index (EVI). All the above methods can facilitate relevant statistical analysis of regional vegetation coverage information. However, in urban areas, the NDVI cannot distinguish vegetation and blue ground objects well, which causes overestimation of vegetation areas, and blue ground objects must be removed (Huang et al., 2023; Yu et al., 2023).

Luoyang is a world-famous tourist city. Currently, an increasing number of tourists not only want information on famous tourist attractions in Luoyang (China) but also want information on the vegetation coverage in the built-up area of Luoyang so that they can better assess the temperature conditions, coordination between vegetation and grey buildings, and likely tourism experience before travelling to Luoyang (Wang et al., 2019). In response to the need of tourists for vegetation coverage information on the Luoyang urban area, in this study, Landsat-8 images were selected for two seasons, i.e., summer and winter, in 2021. The dimidiate pixel model of the NDVI was used to extract vegetation coverage information, after which blue objects were removed using the blue object spectral index. Vegetation coverage classification and transfer analysis of the summer and winter images were conducted to comprehensively grasp the vegetation coverage during the seasons of vigorous vegetation growth and decline in Luoyang, China. The research results could provide data support for improving the perception of tourists of the vegetation coverage in Luoyang, China, which could help dispel certain concerns and convince tourists to visit this well-known tourist city.

Materials and methods

Study area

Luoyang, located in Henan Province, China, is an ancient capital city and a world-famous tourist city. Tourists not only experience the notable historical and cultural atmosphere but also appreciate the famous peony flowers (Ding, 2022). In terms of history and culture, tourists can visit the ancient city of Luoyang, enjoy the elegance of its ancient royal gardens, experience the cultural heritage of the Longmen Grottoes, and appreciate the exquisite art of ancient Chinese stone carvings (Huo, 2023). In terms of

scenery, the peonies in Luoyang are widely known among domestic and foreign tourists (Zhang et al., 2022). Every April, there is a peony flower exhibition, during which tourists flock to Luoyang to admire various peonies species and enjoy their beauty. At present, an increasing number of tourists visit Luoyang, which is becoming a sustainable tourist resort (Zhang et al., 2022c).

Data and preprocessing

The remote sensing data used in this study were captured by the Landsat-8 sensor. The summer and winter data employed in this study were downloaded from <http://www.usgs.gov/>. The imaging times were September 21 (summer) and December 26 (winter) 2021. The two-dimensional grid coordinates of these two datasets (track no. path/row) are 125/36, and the band parameters (the bands considered in this study) are listed in Table 1.

Table 1. Parameters of the three Landsat-8 bands used in this study

Band number	Band name	Wavelength range (μm)	Spatial resolution (m)
4	Red	0.630–0.680	30
5	Near infrared	0.845–0.885	30
8	Panchromatic	0.500–0.680	15

The image range of the two datasets covers the entire urban area of Luoyang. Before mapping the urban vegetation coverage in Luoyang city, we calibrated, fused (i.e., Gram–Schmidt spectral sharpening), and atmospherically corrected (i.e., quick atmospheric correction) the images using ENVI 5.4 software. Then, we applied visual recognition to the image for obtaining the built-up area using tools of interest and cropped the built-up area image (Fig. 1). The built-up area image exhibited latitudinal and longitudinal ranges of 112°17'44.79"–112°36'40.02" E and 34°32'56.42"–34°44'2.14" N, respectively. The area was 359.04 km².

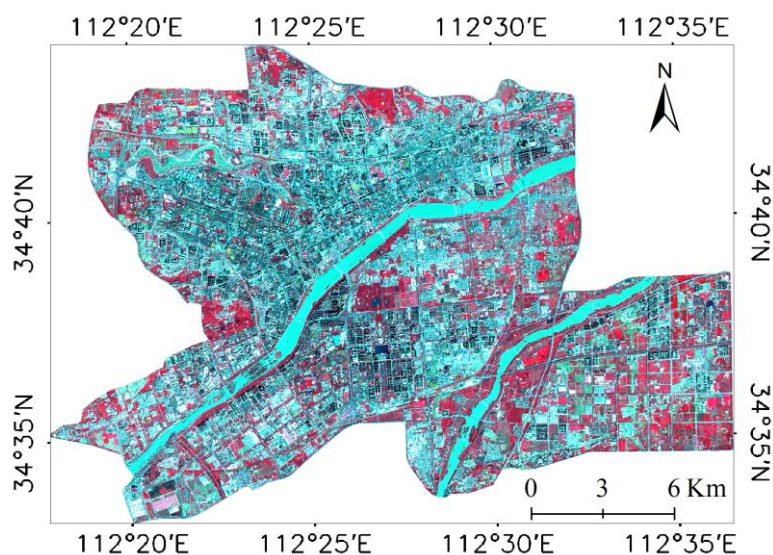


Figure 1. Landsat-8 image (RGB543 combination) of the built-up area of Luoyang (summer image)

Vegetation coverage image extraction

First, we used the near-infrared and red bands to calculate the normalized difference vegetation index (NDVI), and the NDVI can be calculated by *Equation 1*.

$$NDVI = \frac{NIR - R}{NIR + R} \quad (\text{Eq.1})$$

where NDVI is the normalized difference vegetation index, NIR is the near-infrared band, and RED is the red band of the Landsat-8 data.

Then, we introduced the NDVI and its statistical values into *Equation 2* to obtain vegetation coverage images of fc . Many studies have shown that S_{soil} and S_{veg} can be statistically represented by values close to 0 (the NDVI value with a cumulative probability of 5%) and close to the maximum value (the NDVI value with a cumulative probability of 95%), respectively, of the NDVI image (Liu et al., 2018). S was replaced by the NDVI.

$$fc = (S - S_{soil}) / (S_{veg} - S_{soil}) \quad (\text{Eq.2})$$

where fc is the vegetation coverage of a given pixel, S_{veg} is the amount of remote sensing information entirely attributed to the vegetation and S_{soil} is the amount of remote sensing information entirely attributed to the soil.

Therefore, the vegetation coverage can be calculated using the NDVI dimidiated pixel model by *Equation 3*.

$$fc = \frac{NDVI - NDVI_s}{NDVI_v - NDVI_s} \quad (\text{Eq.3})$$

where $NDVI_s$ is the NDVI value of the nonvegetated bare land pixels and $NDVI_v$ is the NDVI value of the vegetated pixels.

Blue ground object removal

Previous studies have shown that blue ground objects in NDVI images exhibit characteristics similar to those of vegetation, and the use of the NDVI only cannot accurately provide vegetation information (Liu and An, 2019). By observing Landsat-8 images in the true colour mode (RGB 432 combination), we identified a large number of blue objects in the built-up area. Therefore, when using the NDVI to extract vegetation, these blue ground objects could be mistakenly extracted as vegetation, resulting in higher vegetation coverage mapping results.

Several researchers have established spectral models using WorldView-2/3 data to accurately extract blue ground objects (Liu and An, 2020; Liu et al., 2020; Liu and Zuo, 2022). Among these models, the BOSI model can be improved to address the impact of blue ground objects on vegetation extraction in this study. In this study, we improved the model, as expressed in *Equation 4*, based on the differences between the band settings of Landsat-8 and WorldView-2/3.

$$NBOSI = (3 \times b_1 + 3 \times b_2 + 3 \times b_6 + 2 \times b_7 - 3 \times b_3 - 4 \times b_4) \times (b_2 - (b_1 + b_3) / 2) \quad (\text{Eq.4})$$

where *NBOSI* denotes the improved blue object spectral index and b_1 , b_2 , b_3 , b_4 , b_6 , and b_7 are the coastal blue, blue, green, red, shortwave infrared 1, and shortwave infrared 2 bands, respectively.

After calculating the *NBOSI*, we selected an appropriate threshold based on the histogram of the pixel distribution of blue ground objects to accurately extract these blue ground objects. Then, we used this threshold to establish a mask and remove blue ground objects from the images of *fc*.

Classification of vegetation coverage grades

Because the vegetation coverage value ranges from 0-100%, we referred to previous research and first selected the appropriate upper bound of the fc_1 value (grade I) to identify nonvegetation areas in the vegetation coverage images (Li et al., 2004; Liu et al., 2018). Then, 100% of the upper bound of the fc_1 value was divided evenly into four equal parts, representing the upper bounds of Grades II, III, IV, and V. The summer and winter vegetation coverage images were categorized using density slices in ENVI 5.4.

Vegetation coverage statistics and change detection

After obtaining vegetation coverage maps of the summer and winter images, coverage areas of different vegetation levels in the images of each season and their proportions in the built-up area were calculated separately. We used the summer and winter vegetation coverage maps as the initial and final state images, respectively, and used ENVI 5.4 to detect changes in the area of vegetation coverage at the different levels. We analysed the vegetation coverage in the built-up area of Luoyang city in summer and winter based on the above statistics, providing basic data for tourists to evaluate the green space conditions in Luoyang.

Results and discussion

Blue ground object removal analysis

As shown in *Figure 2*, both vegetation and blue ground objects are marked with bright colours in the *fc* imagery. Therefore, directly extracting vegetation from *fc* imagery could mistakenly identify blue ground objects as vegetation. The *NBOSI* can enhance the blue ground object signal without enhancing the vegetation signal and can be used to extract blue ground objects and remove them from *fc* imagery. In this study, according to the statistical results, pixels with *NBOSI* values greater than 0.01 were classified as blue ground objects, and their extraction results are shown in *Figure 2e*. We determined that the area of blue ground objects in the built-up area of Luoyang city was approximately 18.94 km². If the blue ground objects in the *fc* images were not removed, the vegetation coverage area in the built-up area would be greatly overestimated.

Vegetation coverage information analysis

The statistical data of the *NDVIs* and *NDVI_v* in summer and winter are listed in *Table 2*. Based on these statistical values, vegetation coverage maps for these two seasons can be accurately extracted.

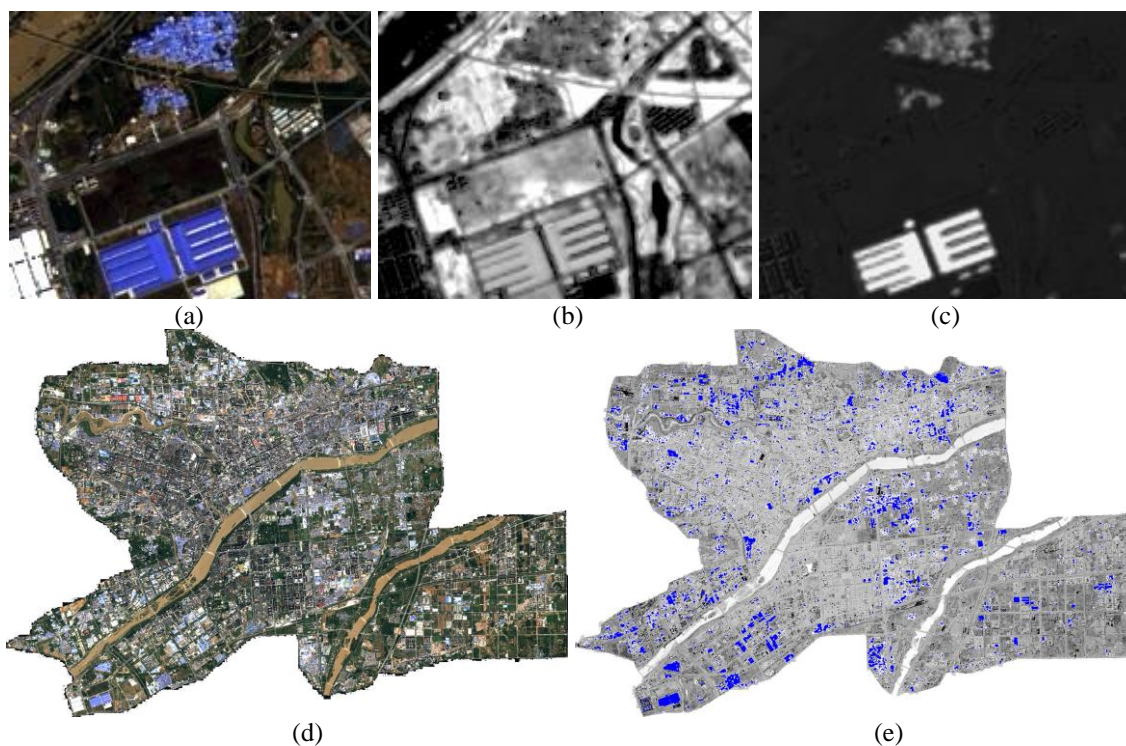


Figure 2. *F_c-based detection results with mistakenly identified blue ground objects as vegetation and detection results of blue ground objects using the NBOSI. (a) Blue ground objects in the summer image (the dark part is vegetation); (b) brightness of the blue ground objects in the f_c image; (c) blue ground objects in the NBOSI image; (d) true colour image of the built-up area in summer; (e) blue object detection results in the image*

Table 2. *Parameter statistical results for calculating coverage maps*

Parameters	Summer	Winter
NDVI _s	0.223529	0.003922
NDVI _w	0.929412	0.615686
Upper bound of f_{c1} for Grade I	20%	20%
Upper bound of f_{c2} for Grade II	40%	40%
Upper bound of f_{c3} for Grade III	60%	60%
Upper bound of f_{c4} for Grade IV	80%	80%
Upper bound of f_{c5} for Grade V	100%	100%

Based on the parameters listed in *Table 2*, using the NDVI pixel dimidiata pixel model, vegetation coverage grade distribution maps for summer and winter of 2021 could be generated, as shown in *Figure 3a* and *b*, respectively, while the vegetation coverage statistics are listed in *Table 3*.

As shown in *Figure 3*, there is a large vegetation area distributed in the built-up area of Luoyang city, and the area covered by vegetation is significantly larger than that the bare area in both summer and winter. However, it is clear that the area covered by vegetation in winter is smaller than that in summer. This indicates that in winter, the shedding of leaves by deciduous trees and withering of grass cause a decrease in the

vegetation coverage area. Although the vegetation coverage area in winter is significantly smaller than that in summer, the vegetation coverage area in the built-up area of Luoyang is still very large in winter.

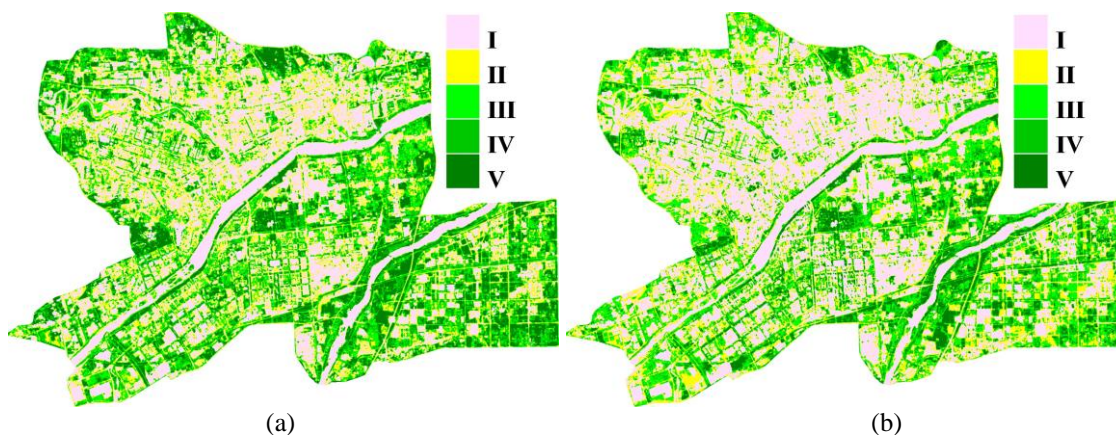


Figure 3. Vegetation coverage grade distribution maps for summer and winter of the built-up area of Luoyang city. (a) Grade vegetation coverage map for summer; (b) grade vegetation coverage map for winter

Table 3. Vegetation coverage statistics for summer and winter

Coverage level	Value range of fc	Summer		Winter		Area change (km ²)
		Area (km ²)	Percentage of the total area (%)	Area (km ²)	Percentage of the total area (%)	
Grade I	$0 \leq fc_1 \leq 0.20\%$	115.93	32.29	142.62	39.72	26.69
Grade II	$20\% < fc_2 \leq 40\%$	73.92	20.59	77.31	21.53	3.39
Grade III	$40\% < fc_3 \leq 60\%$	65.72	18.30	70.13	19.53	4.41
Grade IV	$60\% < fc_4 \leq 80\%$	56.04	15.61	40.55	11.29	-15.49
Grade V	$80\% < fc_5 \leq 100\%$	47.44	13.21	28.44	7.92	-19.00

Table 3 reveals that the total size of the built-up area in Luoyang is 359.04 km². In summer, the vegetation coverage area of Grade I was 115.93 km² (accounting for 32.29% of the total area). The results showed that the proportion of the nonvegetation area in the built-up area of Luoyang was low. Furthermore, the vegetation coverage area of Grade II was 73.92 km² (accounting for 20.59%), the vegetation coverage area of Grade III was 65.72 km² (accounting for 18.30%), the vegetation coverage area of Grade IV was 56.04 km² (accounting for 15.61%), and the vegetation coverage area of Grade V was 47.44 km² (accounting for 13.21%). The vegetation coverage areas of Grades II–V accounted for 67.71% of the total area. This indicates that the vegetation coverage area in the built-up area of Luoyang is very large.

In winter, the vegetation coverage area of Grade I was 142.62 km² (accounting for 39.72% of the total area), the vegetation coverage area of Grade II was 77.31 km² (accounting for 21.53%), the vegetation coverage area of Grade III was 70.13 km² (accounting for 19.53%), the vegetation coverage area of Grade IV was 40.55 km²

(accounting for 11.29%), and the vegetation coverage area of Grade V was 28.44 km² (accounting for 7.92%). The vegetation coverage areas of Grades II–V accounted for 60.28% of the total area. This indicates that in winter, the vegetation coverage area in the built-up area of Luoyang was also very large. However, the area covered by vegetation in winter decreased by 7.43% compared to that in summer.

According to *Table 3*, in summer, the proportion of vegetation coverage levels II, III, IV, and V ranged from 13.21% to 20.59%, with a small difference, and the area showed a decreasing trend. In winter, although the proportions of vegetation coverage levels II, III, IV, and V also exhibited a decreasing trend, the proportion of vegetation coverage level II was nearly three times that of vegetation coverage level V, indicating an imbalance in the proportions of the various vegetation coverage levels. Between summer and winter, the vegetation coverage areas of Grades I, II, III, IV and V changed to 26.69, 3.39, 4.41, –15.49 and 19.00 km², respectively. The vegetation coverage areas of Grades I, II, and III increased, while those of the other grades decreased, indicating that the vegetation coverage transitioned from high levels in summer to low levels in winter.

Vegetation coverage change analysis

Change detection was conducted of the vegetation coverage level maps for summer and winter, and the transfer conditions between the different vegetation coverage levels are summarized in *Table 4*.

Table 4. Grade transfer matrix of the vegetation coverage from summer to winter (%)

Period	Summer					
		Grade I	Grade II	Grade III	Grade IV	Grade V
Winter	Grade I	89.04	42.35	9.09	2.74	1.22
	Grade II	8.87	43.96	36.52	14.66	4.88
	Grade III	1.49	10.77	36.02	39.58	30.77
	Grade IV	0.41	1.67	12.35	29.03	30.47
	Grade V	0.19	1.25	6.03	13.99	32.65
	Class changes	10.96	56.04	63.98	70.97	67.35
	Image difference	23.02	4.56	6.72	-27.64	-40.05

As indicated in *Table 4*, the vegetation coverage areas of Grade I were transferred to Grades II, III, IV and V, accounting for 8.87%, 1.49%, 0.41% and 0.19%, respectively, of the total amount. The change of nonvegetated areas into vegetated areas may be caused by man-made urban greening or the planting of new wheat in autumn. The vegetation coverage areas of Grade II were mainly transformed into Grade I, and very few areas transitioned to higher coverage levels. The vegetation coverage areas of Grades III, IV, and V were also mainly converted into Grades II, III and V with a low vegetation coverage. The results indicated that the vegetation coverage in the built-up area of Luoyang changed from a higher grade in summer to a lower grade in winter.

Travel experience and vegetation coverage

The vegetation coverage in cities in northern China is generally relatively low. For tourists, travelling to cities with a low vegetation coverage suggests that they will

experience extreme heat in summer and may not encounter enough greenery in winter. The mapping of the vegetation coverage in Luoyang in summer and winter showed that the vegetation coverage during both seasons was relatively high (*Fig. 3; Tables 3 and 4*). In summer, a favourable vegetation coverage provides tourists with more opportunities to avoid sun exposure during their travels. Although the vegetation coverage in winter is slightly lower than that in summer, the vegetation coverage is still very satisfactory. In winter, tourists travelling to Luoyang do not have to worry about not being able to enjoy green scenery, which could adversely impact their travel experience. Therefore, when travelling to Luoyang, regardless of the season, a suitable vegetation coverage may increase the travel experience of tourists.

Conclusions

In this study, the vegetation coverage in the built-up area of Luoyang, a world-famous tourist city, was mapped in summer and winter. The purpose was to help tourists better assess the comfort, beauty, leisure and entertainment, health, quality of life and cultural value of the vegetation in this city. The results showed that (1) in summer, the vegetation coverage area in the built-up area of Luoyang was approximately 243.12 km², accounting for 67.71% of the total built-up area, and the proportion of the vegetation area was relatively high; (2) in winter, the area covered by vegetation was approximately 216.43 km², accounting for 60.27% of the total built-up area, and the area covered by vegetation was still very large; and (3) in both summer and winter, the vegetation coverage areas of Grades II, III, IV, and V decreased sequentially. However, the differences were smaller in summer than in winter. (4) In winter, vegetation coverage transitioned from high-level coverage types to low-level coverage types, and the area of the highest-level vegetation coverage type decreased from 47.44 km² in summer to 28.44 km² in winter, representing a decrease of 19 km², reflecting a relatively large reduction.

The results of this study indicated that the vegetation coverage in the famous city of Luoyang is very satisfactory in both summer and winter. Tourists can experience the beauty, coolness, fresh air, and comfort of green vegetation throughout the year.

Acknowledgements. This work was supported by the Scientific and Technological Project of Henan Province (Grant No. 242102320027), the Key Disciplines of Tourism Management in Henan Province, the Collaborative Innovation Center of Smart Tourism in Henan Province, and Henan Province Key R&D and Promotion Project (Soft Science Research) (Grant No. 232400411024). We thank Cheng Jinlong who has contributed to the revision of the paper and partially funded the publication fee through his project. We want to provide our gratitude to the editors and the anonymous reviewers.

Conflict of interest. The authors declare no conflict of interest.

REFERENCES

- [1] Ding, X. (2022): An analysis of Ouyang Xiu's Luo Yang Peony image writing. – Journal of Luoyang Institute of Science and Technology: Social Science Edition 5: 1-7.
- [2] Du, Z., Ma, W., Zhou, Q., Chen, H., Deng-zeng, Z., Liu, J. (2022): Research progress of vegetation recognition methods based on remote sensing technology. – Ecological Science 6: 222-229.

- [3] Huang, L., Yang, Y., Gao, P., Yan, X., You, J., Zhang, H., He, W., Wu, Y. (2023): Temporal and spatial variation of vegetation coverage and its topographical differentiation in the upstream of Minjiang River with Landsat remote sensing image. – *Journal of Northeast Forestry University* 1: 54-60.
- [4] Huang, Y., Xie, Y., Tang, X., Wang, J. (2011): Research and implementation of cooperative information system for forest and greening inventory in Beijing. – *Journal of Zhejiang A & F University* 6: 884-892.
- [5] Huo, H. (2023): On the Sui-Tang Luoyang City related to the Longmen grottoes in space and geography. – *Palace Museum Journal* 3: 34-53.
- [6] Li, M., Wu, B., Yan, C., Zhou, W. (2004): Estimation of vegetation fraction in the upper basin of Miyun Reservoir by remote sensing. – *Resource Science* 26(4): 153-159.
- [7] Li, X., Lei, S., Feng, J., Wen, Y. (2019): Assessing the value of cultural ecosystem services in urban green space of Beijing. – *Journal of Arid Land Resources and Environment* 33(6): 33-39.
- [8] Liu, H., An, H. (2019): Urban greening tree species classification based on HSV colour space of WorldView-2. – *Journal of the Indian Society of Remote Sensing* 47(11): 1959-1967.
- [9] Liu, H., An, H. (2020): Extraction of four types of urban ground objects based on a newly created WorldView-2 multi-colour spectral index. – *Journal of the Indian Society of Remote Sensing* 48(7): 1091-1100.
- [10] Liu, H., Zuo, X. (2022): Extraction of blue roofs using BRSAM and the newly created spectral index derived from WorldView-2/3 imagery. – *Heliyon* 8(9): e10417.
- [11] Liu, H., Zhang, Y., Zhang, X. (2018): Monitoring vegetation coverage in Tongren from 2000 to 2016 based on Landsat 7 ETM+ and Landsat 8. – *Anais da Academia Brasileira de Ciências* 90(3): 2721-2730.
- [12] Liu, H., Zhang, Y., An, H. (2020): Urban blue ground object extraction by using a new spectral index from WorldView-2. – *Fresenius Environmental Bulletin* 29(11): 9654-9660.
- [13] Liu, J., Fan, J., Yang, C., Xu, F., Zhang, X. (2022b): Novel vegetation indices for estimating photosynthetic and non-photosynthetic fractional vegetation cover from Sentinel data. – *International Journal of Applied Earth Observation and Geoinformation* 109: 102793.
- [14] Liu, Y., Cai, X., Ning, X., Wang, H. (2022a): Research on urban forest mapping based on landscape ecological index model. – *Science of Surveying and Mapping* 11: 185-195.
- [15] Luo, Q. (2019): The Influence of Plant Landscape on Tourists' Perceived Value: Based on the Experience of the West Lake Scenic Area. – Zhejiang Gongshang University, Zhejiang.
- [16] Wang, C., Huang, S., Deng, M., Wei, W. (2023): Research on equity of park green spaces in high-density cities from the perspective of supply-demand coupling coordination: a case study of Longhua District, Shenzhen. – *Chinese Landscape Architecture* 1: 79-84.
- [17] Wang, Y., Zhang, J., Zhang, M., Cui, H. (2019): Contrastive analysis of thematic image projection and perception in Luoyang Botanical Garden of Sui and Tang Dynasties. – *Journal of Southwest China Normal University (Natural Science)* 44(7): 101-109.
- [18] Yu, T., Pang, Y., Meng, S., Jia, W., Li, H., Sun, B. (2023): Remote sensing estimation and change analysis of fractional vegetation coverage in Natural Forest Resource Protection Project area. – *Journal of Beijing Forestry University* 5: 1-13.
- [19] Zhang, H., Ying, S., Wu, M. (2022a): Topic identification and asymmetry effects of tourists' perceived image of cultural tourism destinations: a case of canal city Shaoxing. – *Scientia Geographica Sinica* 42(12): 2131-2140.
- [20] Zhang, T., Lin, S., Wang, C. (2022c): Research on design and development of the intangible heritage IP cultural derivative products--exemplification with Luoyang Peony Fair. – *Culture & Communication* 6: 62-66.

- [21] Zhang, Y., Liu, T., Tong, X., Duan, L., Jia, T., Ji, Y. (2022b): Inversion of vegetation coverage based on multi-source remote sensing data and machine learning method in the Horqin Sandy Land, China. – *Journal of Desert Research* 3: 187-195.